Correction of Beam Steering for Optical Measurements in Turbulent Reactive Flows

Ke Zhou, Lin Ma* (Do NOT enter this information. It will be pulled from participant tab in MyTechZone)

Affiliation (Do NOT enter this information. It will be pulled from participant tab in MyTechZone)

Abstract

The application of optical diagnostics in turbulent reactive flows often suffers from the beam steering (BS) effects, resulting in degraded image quality and/or measurement accuracy. This work investigated a method to correct the BS effects to improve the accuracy of optical diagnostics, with particle imagine velocimetry (PIV) measurements on turbulent reactive flames as an example. The proposed method used a guiding laser to correct BS. Demonstration in laboratory turbulent flames showed promising results where the accuracy of PIV measurement was significantly enhanced. Applicability to more complicated and practical situations are discussed.

Introduction

The application of optical diagnostics in turbulent reactive flows often suffers from the beam steering (BS) effects[1-6]. The BS effect refers to the refraction of the signal due to the refractive index gradients inherent in turbulent flames [7-9]. Such refraction can lead to degraded image quality and/or measurement accuracy[10; 11], with particle image velocimetry (PIV) measurements as a representative example. PIV has been demonstrated as a powerful tool to study both reactive and non-reactive flows[12-14]. Conceptually, PIV obtains 2D velocity fields by cross-correlating two particle images captured at consecutive times. However, when PIV is applied to reactive flows, the BS effects can significantly impair the PIV accuracy by distorting the particle images[15], and subsequently introduce uncertainties into the cross-correlation and the end velocity measurements[1; 16].

Even though the BS issue is well recognized, its correction is challenging because the BS effects vary both spatially and temporally due to the stochastic nature of turbulent flames. A few efforts have been invested to investigate the correction of the BS effects in PIV measurements, for example, in tomographic PIV measurements [17; 18]. Essentially, the idea involved exploiting the multi-camera configuration used in tomographic PIV [19-21]. With multiple cameras available from different views, each camera would experience a different distortion, the position of the particles then could be corrected by finding a best match between their back-projections and the measured particle images for all views. The corrected particle reconstructions at two consecutive frames can then be cross-correlated to obtain velocity with improved accuracy. The quantitative nature of such correction merits further investigation.

An alternative method is desired in applications where a multi-camera configuration is infeasible (either due to equipment or optical access restriction). This paper therefore reports the investigation of a new method, referred to as the laser line method, to correct the BS effects

Page 1 of 6

10/20/2020

and improve the accuracy of PIV measurements. The method utilizes a reference laser line to monitor the BS effects simultaneously with the PIV measurement. The rest of the paper is organized as follows. The next session describes the correction method and its demonstration using a controlled experimental. Then section 3 discusses the results with accompanying analysis. Finally, the last section summarizes the paper and discusses the method's potential applications, its current limitations, and future work.

Correction Method and Demonstration Experiment

This section describes the method and also the experimental setup to demonstrate it using the schematic shown in Fig. 1. Conceptually, the laser line method corrected the BS effects by generating a reference laser line within the PIV measurement domain (as illustrated by the red vertical line in the center of Fig. 1). The reference laser line then was used to track the BS effects in situ by the variation in its shape (it should be a straight line without any BS effects). Information about the BS effects provided by the laser line were then used to correct the measured particle scattering signals before the cross-correlation.

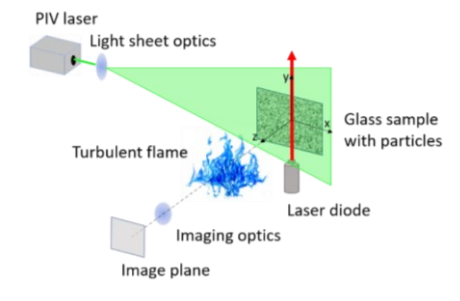


Figure 1. Experimental setup

To demonstrate the above concept, a controlled experiment was designed as shown in Fig. 1. A key of such experiment is to generate a controlled velocity field known a priori with sufficient precision, so that the effects of BS and the subsequent correction could be quantified. Our solution involved a solid glass sample embedded with tracer particles [21; 22]. The sample was then mounted on a stage, and by controlling the movement of the stage, precise velocity fields can be created. The remainder of the setup consisted of a PIV laser, a camera, a burner, and a laser diode that served as the reference laser as shown in Fig. 1.

Commented [ML(1]: Overall comments:

- 1. Ning will not be a co-author anymore
- 2. proofread again
- 3. check the formatting of the references. I may have messed them
- up. 4. are u sure this is the correct template? Chris is using a different one for his paper. Check with him.

Commented [KZ2R1]: All done.

As shown, the glass sample was vertically mounted on a stage to create the controlled velocity fields. The sample had a physical dimension of 150 mm \times 100 mm \times 0.5 mm in height, width and thickness, and was coated with polystyrene particles of an average diameter of 4.05 μm on its surface. The stage (OptoSigma TSD-602C) that held the glass could translate with 10 μm precision, a precision significantly beyond the accuracy of PIV technique. A Cartesian coordinate system was established with the origin fixed at the center of the glass sample, and the x,y, and z axes were defined along its width, height and thickness direction, respectively, as shown.

The PIV laser was a CW laser (Edmund Optics, PGL-532/1064) with a wavelength of 532 nm. The laser output was expanded by a cylindrical lens to a thin laser sheet to illuminate the particles on the glass sample, generating scattering signals to be captured by the camera for the PIV measurements. The camera (Photron SA-4) was aligned perpendicular to the glass sample. The distance from the lens to the glass sample was measured to be 324 mm. The camera was equipped with a 105 mm Nikon lens, and the magnification ratio was 0.48. All experiments were operated at an exposure time of 2ms.

A Bunsen burner was placed between the sample and the camera. The burner generated a turbulent propane-air flame to cause BS effects to the scattering signals. The distance between the burner and the glass sample was ~60 mm. The turbulent flame operated at a Reynolds number of 6240 defined based on the slot length (40 mm). The flame had a physical dimension of ~40 mm (width) × ~40 mm (height) × ~15 mm (depth), large enough to cause BS effects to most, if not all, of the measurement region.

The last component in the setup was the reference laser. A laser diode (635 nm, Edmund Optics, Micro LDM 57-101) was used to generate a laser line along the z axis as shown. The laser line was aligned through the center of the glass sample. The laser line was focused and collimated to have a diameter of $\sim\!0.3$ mm (i.e., 6 pixels on images) in the measurement region.

With the above experimental setup, the laser line correction method was demonstrated in the following five steps. First, before any experiments, a BS-free laser line image was captured without the flame to provide a reference position of the laser line. Second, with the flame turned on, a BS-contaminated particle image was captured by the camera, together with the laser line simultaneously captured in the image. Third, the glass sample was moved by a controlled distance using the stage, and the second BS-contaminated particle image was captured by the camera, again with the laser line simultaneously captured. Fourth, this is the step where the BS correction was performed to the images captured in steps 2 and 3. At each pixel row in both BS-contaminated and BS-free laser line images, the horizontal pixel intensity distribution was fitted with a spline curve to locate the peak intensity position with sub-pixel accuracy. Then, at each pixel row, the difference of peak intensity positions for BS-contaminated and BS-free laser line images was calculated. By combining the differences at all pixel rows, the horizontal BS-caused image displacements can be inferred along the vertical laser line. With the inferred image displacements, the BS-distorted particle images (i.e., those obtained in steps 2 and 3) were corrected by shifting the particles on the image along the opposite direction of the inferred image displacements. The fifth and last step, performed a cross-correlation using the two corrected particle images obtained in step 4 to obtain the velocity field.

Page 2 of 6

10/20/2020

Results and Discussions

With the above experimental setup, a series of controlled PIV measurements were performed to demonstrate the proposed laser line method. Figure 2 summarizes a set of measurements obtained with a 0.5 mm horizontal movement of the sample (corresponding to a displacement of 12 pixels on the image). The results here show a total of 7×15 velocity vectors in a region adjacent to the reference laser line (shown by the red vertical arrow). These results were obtained by cross-correlating the two particle images (with a pixel resolution of 192×400) before and after the movement of the solid sample as aforementioned, with an interrogation window of 48×48 pixels at 50% overlap. Figure 2a first shows the ground truth velocity field in the controlled measurement (which was a uniform displacement of 12 pixels). Fig. 2b-d then show the measured velocity fields to be compared with Fig. 2a to quantify the accuracy improvement brought about by the laser line method.

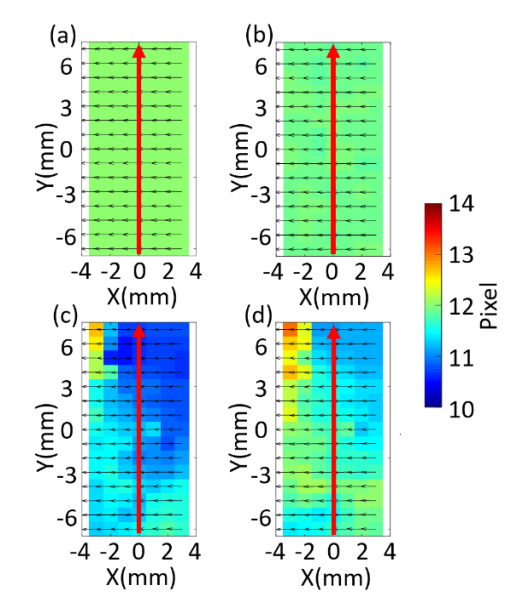


Figure 2. Controlled PIV measurements, with the color scale representing velocity vector magnitudes, and the arrows the velocity vectors. The red vertical arrow represents the reference laser line. (a) Ground truth velocity field, b) BS-free velocity field measured with the flame off, (c) velocity field measured with the flame turned on and without correcting the BS effects, (d) velocity field obtained after correcting for the BS effects.

Fig. 2b shows the velocity field measured without any BS effects (with the flame off) to provide an assessment of the PIV measurement itself. As can be seen, without any BS effects, the PIV measurement accurately captured the true velocity field, with the velocity vector magnitudes uniformly distributed across the entire measurement domain. Fig. 2c shows the velocity field measured with BS effects (with the flame on) but without any correction, i.e., Fig. 2c was obtained by directly cross-correlating the two BS-distorted particle images. As seen in Fig. 2c, the velocity vector magnitudes are non-uniformly distributed, illustrating the BS effects created by the

turbulent flame. Finally, Fig. 2d shows the velocity field after the BS effects were corrected by the laser line method. As mentioned in section 2, the BS correction was performed by correcting both BS-distorted particle images, which were then cross-correlated to obtain the velocity field with enhanced accuracy. As seen in Fig. 2d, the velocity vectors were closer to the ground truth (in Fig. 2a) than those of the uncorrected velocity field (in Fig. 2c), demonstrating the effectiveness of the laser line method for BS correction.

To quantitatively assess the performance of the laser line method seen above, a few quantitative metrics were defined. First, the average velocity error (e_v) was defined as

$$e_{v} = \frac{\sum |V - V_{true}|}{\sum |V_{true}|} \tag{1}$$

where V and V_{true} represent the measured and ground truth velocity fields, respectively. The | | denotes the modulus of a vector, and the summation operated on a vector-by-vector basis across the entire measurement domain. The definition of e_v in Eq. 1 represents an averaged discrepancy between the measured value and true value, combining both errors due to velocity magnitude and the velocity direction [23]. To decouple such combination so that the error in velocity direction can be isolated, an average velocity direction error (denoted as e_d) was also defined. The definition is similar to Eq. (1), except the discrepancy between the direction of the measured velocity fields and the ground truth was used. The e_v and e_d of the measurements shown in Fig. 2b-d are summarized in Table 1 below. As seen from Table 1, the laser line method reduced the error caused by the BS effects, in terms of both e_v and e_d . Especially in terms of e_v , the laser line method was able to substantially reduce the e_v of the BS-contaminated PIV measurement from 7.2% to 3.8%, resulting in an accuracy improvement by ~47%. Also note that the e_v of 3.8% is still significantly higher than that of the measurement without any BS effects (i.e., 0.7%), suggesting that there is still potential to improve the correction method.

Table 1. Errors of velocity measurements under different conditions

	BS-free measurement	With BS effect but no correction	BS effect correct by laser line method
e_v	0.7%	7.2%	3.8%
e_d	0.3°	0.9°	0.8°

As mentioned above, the BS effects caused by turbulent flames vary spatially across the measurement domain as seen from Fig. 2c, posing a great challenge to the development of the correction method. To investigate the extent of the measurement area that can be effectively corrected by a single laser line under such spatial variation, the laser line method was applied to regions with various dimensions adjacent to the laser line. Figure 3 shows the correction results when the laser line method was applied to a large PIV measurement region that was of various distance from the laser line itself. The region had a dimension of 16 mm (in the X direction) × 14 mm (in the Y direction), and the distance of the region from the laser line varied from 1 to 7 mm. Figure 3 shows the velocity error distributions (i.e., e_v) of the uncorrected and corrected BS-contaminated velocity fields as a function of the distance to the laser line (at X = 0). The results in Fig. 3 were obtained using the same measurement procedure and the same computational settings (i.e., interrogation window size and step size) as those in Fig 2c and 2d. As shown in Fig. 3, the e_v for the uncorrected velocity field fluctuated around 6%~7% in all cases. By contrast, the corrected velocity field exhibited a significantly lower e_v of around 3%~4% in the measurement area within a distance of 4 mm to the laser Page 3 of 6

10/20/2020

line. Beyond the distance of 4 mm, the corrected velocity errors began to approach the uncorrected counterparts, and the effectiveness of the BS correction method diminished. This set of results demonstrated the laser line's ability to only correct the BS effects in its adjacent measurement area due to the inherent spatial variation of turbulence-caused BS effects. The extent for the method to be effective was around 8 mm (i.e., 4 mm at each side of the laser line) for the settings used in this work. More discussions of this challenge and further work to overcome it will be presented in the summary section.

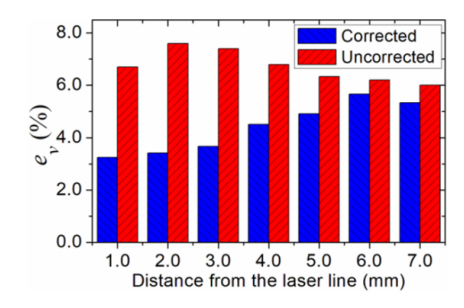


Figure 3. Error of the corrected and uncorrected velocity fields with varying distances from the laser line.

After the above illustration of the laser line's ability and limitation to improve the accuracy of velocity measurements in the presence of BS effects, here we present some intermediate results, as shown in Fig. 4 and 5, in the correction process to provide insights into the correction method. As mentioned in Section 2, the method corrected the particle image distorted by the BS effects using the displacements inferred from the laser line. Such particle image correction was essentially based on the laser line's ability to approximate the BS effects experienced by its nearby particles with the inferred image displacements. To confirm this ability, Fig. 4 compares the inferred image displacements and the adjacent particle position errors caused by the BS effects (as a reflection of the particles' BS effects), using the first frame of the PIV measurement in Fig. 2c as an example.

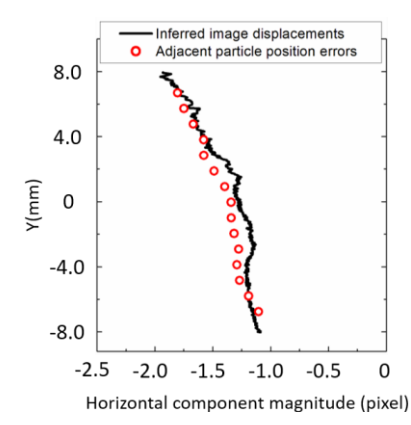


Figure 4. Comparison of the horizontal components of the inferred image displacements and the adjacent particle position errors.

As seen in Fig. 4, the black line and the red circles represent the horizontal component magnitudes of the inferred image displacements and the adjacent particle position errors, respectively, both of which are plotted along the Y direction of the measurement domain. Specifically, the inferred image displacements were obtained by calculating the laser line's horizontal position variation due to the BS effects at each pixel row of the image, as mentioned in Section 2. And the adjacent particle position errors were obtained by cross-correlating the particle images with and without BS effects within an interrogation window (48×48 pixels) centered at different heights of the laser line, such that only position errors of particles within this adjacent interrogation window were taken in account. As seen in Fig. 4, the inferred image displacements match well with the adjacent particle position errors in terms of their horizontal component magnitudes. Quantitatively, the averaged horizontal component magnitudes of the inferred image displacements and adjacent particle position errors at all heights are -1.37 pixels and -1.44 pixels, with a relative difference of ~5%. This comparison indicates the correction method's ability to infer the adjacent particle position errors induced by the BS effects. Note that the difference of ~5% could be explained by the spatialaveraging nature of the cross-correlation to obtain the adjacent particle position errors (i.e., within an interrogation window of 48×48 pixels), while the laser line inferred image displacements in a pixel-wise fashion (i.e., at each pixel row). Nevertheless, the error in the final velocity field caused by this ~5% difference was negligible compared to that caused by the BS effects.

Fig 5 further demonstrates the correction of the BS-distorted particle image (as the basis of the above velocity field correction in Fig. 2), again using the example of the first frame of the PIV measurement in Fig. 2c. As mentioned in Section 2, the image correction was implemented by shifting the particle image along the opposite direction of the inferred image displacements, such that the image distortion due to the BS effects can be compensated. To visualize the image correction process, both the uncorrected and corrected particle images under the BS effects are overlaid onto the BS-free particle image for comparison, as shown in Fig. 5a and 5b. In Fig. 5a, the red and green dots represent the uncorrected particle image (with BS effects) and the BS-free particle image, respectively. As seen in Fig. 5a, the uncorrected particles (in red) clearly deviated from their real positions (shown in green) by 1~2 pixels due to the BS effects. Fig. 5b shows the corrected particle image obtained by the laser line method, and the particles after correction are shown in blue. The particle image measured without the BS effects are again overlaid in Fig. 5b in green. However, the green almost cannot be seen from Fig. 5b, because the corrected particles (in blue) almost overlapped entirely with the BSfree ones (in green), providing a visual confirmation of the effectiveness of the correction method.

Fig. 5c and 5d show the particle position error distributions over the entire measurement domain for the uncorrected and corrected particle images (with BS effects), respectively. In Fig. 5c, the uncorrected particle position error distribution was obtained by cross-correlating the uncorrected particle image (red in Fig. 5a) with the BS-free one (green in Fig. 5a). Again, the computational settings (i.e., the interrogation window size and step size) were the same as those used for velocity field calculation in Fig. 2. Here, the uncorrected particle position error vectors are non-uniformly distributed across the entire measurement domain in terms of both the magnitude and direction, illustrating the complex BS effects generated by the turbulent flame. The uncorrected particle position error magnitude averaged across the entire measurement domain was calculated to be 1.51 pixels, causing a significant uncertainty into the subsequent velocity calculation. Fig. 5d illustrates the corrected particle position error distribution obtained

Page 4 of 6

10/20/2020

by cross-correlating the corrected particle image (blue in Fig. 5b) with the BS-free one (green in Fig. 5b), using the same computational settings as in Fig. 5c. As seen, the error vectors now are significantly smaller than those from the uncorrected images. The corrected particle position error magnitude averaged across the entire measurement domain was calculated to be 0.47 pixel, substantially lower than the uncorrected one of 1.51 pixels (a reduction of ~68%). Furthermore, the error is now mostly only in the vertical direction, and this is due to the vertical laser line's correction ability only existed along the horizontal direction. As a result of such ability to correct the BS effects, the laser line method was able to significantly enhance the accuracy of the PIV measurements as shown in Fig. 2d. Lastly, note that the error of 0.47 pixel seen here were mostly in the vertical direction (which as aforementioned, was due to the vertical laser line used in this work). The effectiveness of the method could be further enhanced if another laser line is also used (for example, at an orthogonal orientation).

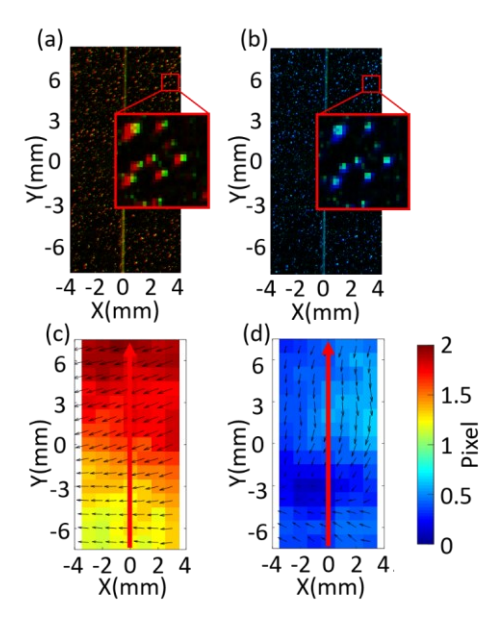


Figure 5. (a) uncorrected particle image with BS effects (red) overlaid on the image without BS effects (green). (b) corrected particle image with BS effects (blue) overlaid on the image without BS effects (green). (c) and (d) particle position error distributions for the uncorrected (red in panel (a)) and the corrected particle images (blue in panel (b)), with the color scale representing the error magnitudes, and the black arrows the error vectors. The vertical red arrow represents the laser line.

Summary and Discussions

This work reports the investigation of a novel method to correct the beam steering (BS) effects in optical diagnostics when applied to turbulent reactive flows. The method uses a reference laser line to track the BS effects in situ and subsequently corrects them. The method was demonstrated in controlled PIV measurements using turbulent flames and was shown to be effective. A set of controlled PIV measurements were designed using a solid sample embedded with tracer particles so

that precisely controlled velocity fields can be generated and can be used to quantify the effectiveness of the correction method. In the demonstration experiments, the laser line method was shown to reduce the displacements of particle positions caused by BS effects by ~68%, which ultimately improved the accuracy of BS-contaminated PIV measurements by ~47%, compared to measurements without any correction of the BS effects. These results suggest the method as a promising approach to address the long-standing issue of quantitative optical measurements in practical environments.

Several future research directions are also recognized from this current study. First, as mentioned, each reference laser line can only provide information to accurately correct the BS effects in its adjacent measurement area (as illustrated in Fig. 3). This is because the BS effects vary spatially due to inherent non-uniformity of turbulent reactive flows. To correct the BS effects in a larger measurement area (or a volume), multiple laser lines can be used and it is straightforward to apply the same method described in this work to each of them and correct for the entire area (or volume). Second, a reference laser line can only provide information to correct the BS effects in one direction (the direction normal to the laser line). The results in this work showed that even with this limitation, the information provided by one laser line can already significantly reduce the error caused by BS. The effectiveness of the correction could be further enhanced if another laser line (or multiple of them) are used from different orientations. Note that the use of multiple laser lines can address both the first and second topic mentioned (i.e., a grid formed by multiple laser lines can be envisaged to correct the BS effects in a large area or volume in all three spatial directions). And also note that in practical implementations, the multiple laser lines could be generated with one laser by using mirrors to reflect it multiple times or by fiber optics.

References

- Stella, A., G. Guj, J. Kompenhans, M. Raffel, and H. Richard. 2001. "Application of particle image velocimetry to combusting flows: design considerations and uncertainty assessment." Experiments in Fluids 30 (2): 167-180.
- Cai, Weiwei, and Lin Ma. 2012. "Improved Monte Carlo model for multiple scattering calculations." *Chinese Optics Letters* 10 (1): 012901.
- Webber, Michael E, Jian Wang, Scott T Sanders, Douglas S Baer, and Ronald K Hanson. 2000. "In situ combustion measurements of CO, CO2, H2O and temperature using diode laser absorption sensors." Proceedings of the Combustion Institute 28 (1): 407-413.
- Zhao, Yan, Xuesong Li, and Lin Ma. 2012.
 "Multidimensional Monte Carlo model for two-photon laser-induced fluorescence and amplified spontaneous emission."
 Computer Physics Communications 183 (8): 1588-1595.
- Sanders, Scott T, Jeffrey A Baldwin, Thomas P Jenkins, Douglas S Baer, and Ronald K Hanson. 2000. "Diode-laser sensor for monitoring multiple combustion parameters in pulse detonation engines." *Proceedings of the Combustion Institute* 28 (1): 587-594.
- Kruse, S, PR Medwell, J Beeckmann, and H Pitsch. 2018.
 "The significance of beam steering on laser-induced incandescence measurements in laminar counterflow flames." Applied Physics B 124 (11): 212.
- Kaiser, S. A., J. H. Frank, and M. B. Long. 2005. "Use of Rayleigh imaging and ray tracing to correct for beam-

- steering effects in turbulent flames." Applied Optics 44 (31): 6557-6564.
- Wang, Shengkai, and Ronald K Hanson. 2018. "Ultrasensitive spectroscopy of OH radical in high-temperature transient reactions." Optics letters 43 (15): 3518-3521.
- Hemmerling, Bernd. 1997. "Beam-steering effects in turbulent high-pressure flames." Combustion Diagnostics.
- 10. Peng, Wen Yu, Séan J Cassady, Christopher L Strand, Christopher S Goldenstein, R Mitchell Spearrin, Christopher M Brophy, Jay B Jeffries, and Ronald K Hanson. 2019. "Single-ended mid-infrared laser-absorption sensor for time-resolved measurements of water concentration and temperature within the annulus of a rotating detonation engine." Proceedings of the Combustion Institute 37 (2): 1435-1443.
- Hanson, Ronald K, R Mitchell Spearrin, and Christopher S Goldenstein. 2016. Spectroscopy and optical diagnostics for gases. Springer.
- Raffel, M., C. E. Willert, S. T. Wereley, and J. Kompenhans. 2007. "Particle Image Velocimetry: A Practical Guide, Second Edition." Particle Image Velocimetry: A Practical Guide, Second Edition: 1-448.
- Mungal, M. G., L. M. Lourenco, and A. Krothapalli. 1995.
 "Instantaneous velocity measurements in laminar and turbulent premixed flames using on-line PIV." Combustion Science and Technology 106 (4-6): 239-265.
- Sun, ZW, ZT Alwahabi, DH Gu, SM Mahmoud, GJ Nathan, and BB Dally. 2015. "Planar laser-induced incandescence of turbulent sooting flames: the influence of beam steering and signal trapping." Applied Physics B 119 (4): 731-743.
- Ertem, C., J. Janicka, and A. Dreizler. 2012. "Ray tracing of chemiluminescence in an unconfined non-premixed turbulent jet flame using large-eddy simulation." Applied Physics B-Lasers and Optics 107 (3): 603-610.
- Muniz, L, RE Martinez, and MG Mungal. 1997.
 "Application of PIV to turbulent reacting flows." In Developments in Laser Techniques and Fluid Mechanics, 411-424. Springer.
- 17. Weinkauff, J., D. Michaelis, A. Dreizler, and B. Bohm. 2013. "Tomographic PIV measurements in a turbulent lifted jet flame." Experiments in Fluids 54 (12)
- jet flame." Experiments in Fluids 54 (12).

 18. Wieneke, B. 2008. "Volume self-calibration for 3D particle image velocimetry." Experiments in Fluids 45 (4): 549-556.
- Liu, Ning, and Lin Ma. 2020. "3D flame measurements using tomography reconstruction integrating view registration." AIAA Scitech 2020 Forum.
- Liu, Ning, Ke Zhou, and Lin Ma. 2020. "3D tomography integrating view registration and its application in highly turbulent flames." Combustion and Flame 221: 429-440.
- Liu, Ning, and Lin Ma. 2020. "Regularized tomographic PIV for incompressible flows based on conservation of mass." Applied Optics 59 (6): 1667-1677.
- Liu, Ning, Yue Wu, and Lin Ma. 2018. "Quantification of tomographic PIV uncertainty using controlled experimental measurements." Applied optics 57 (3): 420-427.
- Stark, Matthew. 2013. "Optical Flow PIV: Improving the Accuracy and Applicability of Particle Image Velocimetry." ETH, Department of Mechanical and Process Engineering.

Contact Information

Ke Zhou, PhD student.

Department of Mechanical and Aerospace Engineering, University of Virginia, Charlottesville, VA Email: kz4nm@virginia.edu

Lin Ma, PhD, Professor Department of Mechanical and Aerospace Engineering, University of Virginia, Charlottesville, VA Email: linma@virginia.edu

Acknowledgment

This work is supported by the National Science Foundation (Award Number: 1839603). And the authors thank Dr. Ning Liu for his assistance with the demonstration experiment.

Page 6 of 6 $\,$

10/20/2020